pH-Sensitive Supramolecular Polypeptide-Based Micelles and Reverse Micelles Mediated by Hydrogen-Bonding Interactions or Host−Guest Chemistry: Characterization and In Vitro Controlled Drug Release

Yi Chen and Chang-Ming Dong*

Department of Polymer Science & Engineering, School of Chemistry and Chemical Engineering, Shanghai Jiao Tong University, Shanghai 200240, P. R. China

Received: January 15, 2010; Revised Manuscript Received: March 3, 2010

A versatile strategy is provided for the fabrication of pH-sensitive polypeptide-based normal micelles and reverse micelles from the same polypeptide-based copolymers via hydrogen-bonding interactions or host−guest chemistry. The pH-sensitive self-assembly of both linear and dendron-like/linear poly(L-glutamic acid)-*b*-poly(ethylene oxide) (Dm-PLG-*b*-PEO) block copolymers was investigated in detail by means of UV−vis, dynamic light scattering, NMR, fluorescence spectroscopy, and transmission electron microscopy. It was demonstrated that both the copolymer topology and the composition controlled the morphology of the polypeptide-cored normal micelles. Importantly, a novel class of polypeptide-shelled reverse micelles was for the first time generated by host−guest-chemistry-mediated self-assembly of these copolymers and α-cyclodextrin (α-CD) in alkaline solution. The supramolecular inclusion complexation between PEO and α-CD was confirmed by wide-angle X-ray diffraction, differential scanning calorimetry, and NMR. Moreover, the ζ potential of the reverse micelles ranged from −20.2 to −24.2 mV, convincingly demonstrating that the reverse micelles had an anionic PLG shell. Furthermore, the anticancer doxorubicin (DOX)-loaded micelles fabricated from the dendron-like/linear copolymer showed a higher DOX loading efficiency (38%) and capacity (24%) and sustained a longer drug-release period (∼70 days) than the linear counterpart. Consequently, this will provide a platform for the fabrication of supramolecular polypeptide-cored and polypeptide-shelled micelles for the anticancer drug delivery systems.

Introduction

Owing to the prolonged blood circulation time, durable stability, the enhanced permeability and retention (EPR) effect, and especially tunable physicochemical and biological surfaces, polymeric micelles and vesicles (or polymersomes) have been increasingly investigated for molecular diagnosis and drug/gene/RNA delivery systems in comparison with small molecular surfactant micelles and liposomes.[1−8] Generally speaking, polymeric micelles and vesicles can be easily fabricated by the following four main strategies: (a) the aqueous self-assembly of amphiphilic block and graft copolymers through the hydrophobic interactions among the core-forming segments; (b) the so-called polyion complex micelles assembled from the electrostatic interactions of water-soluble polyelectrolyte/ionomer-containing copolymers; (c) the aqueous self-assembly of double hydrophilic block copolymers tuned by environmental stimulus, such as pH and temperature; and (d) the supramolecular assemblies mediated by specific supramolecular interactions, such as molecular recognition and host−guest chemistry.[1−13]

Biocompatible cyclodextrins with a hydrophobic and hollow truncated cavity can thread along various polymer backbones to form a variety of polypseudorotaxanes, which are mainly driven by the geometric size, the hydrophobic interactions between cyclodextrins and polymers, and the hydrogen-bonding interactions among cyclodextrins.[14−18] For example, increasing efforts were being made on the preparation of various polypseudorotaxane-based materials for drug/gene delivery systems.[19−23] However, fabricating polypseudorotaxane-based micro- and nanoparticles is still challenging because of the insolubility of polypseudorotaxanes in common organic solvents and especially in water.[21−23]

Synthetic polypeptide or protein hybrid copolymers, so-called "molecular chimeras", recently received much attention for the fabrication of stimuli-responsive micelles and vesicles for various biomedical applications, such as drug delivery and gene therapy.[3,4,24−31] In particular, intensive efforts are being made on the hierarchical self-assembly of synthetic polymer−polypeptide block copolymers with varying hydrophobic blocks as well as varying the amino acids in the polypeptide blocks.[32−46] It was demonstrated that both the conformational structure (e.g., random coil and α-helix) and the copolymer composition controlled the morphology and size of self-assembled nanostructures.[37−46] However, the aqueous self-assembly of dendritic or branched polypeptide hybrid copolymers is rarely studied, which might provide a platform for developing multifunctional and stimulus-responsive drug delivery vesicles.[47,48]

Very recently, a series of dendron-like polypeptide/linear poly(ethylene oxide) block copolymers was synthesized by utilizing click chemistry, and the supramolecular polypeptide-based hydrogels were fabricated by host−guest chemistry.[49,50] Herein we report the pH-sensitive supramolecular polypeptide-based normal and reverse micelles, which were generated from both linear and dendron-like/linear poly(L-glutamic acid)-*b*-poly(ethylene oxide) (Dm-PLG-*b*-PEO, $m = 0$ and 3) block copolymers by utilizing hydrogen-bonding interactions or host−guest chemistry, as shown in Scheme 1. The pH-sensitive self-assembly of the Dm-PLG-*b*-PEO copolymers was thor-

* Corresponding author. Tel: 86-21-54748916. Fax: 86-21-54741297. E-mail: cmdong@sjtu.edu.cn.

10.1021/jp100399d
Published on Web 05/14/2010

SCHEME 1: Aqueous Self-Assembly of (a) the Polypeptide-Based Normal Micelles and (b) Reverse Micelles Generated from the Dm-PLG-*b*-PEO Copolymers[a]

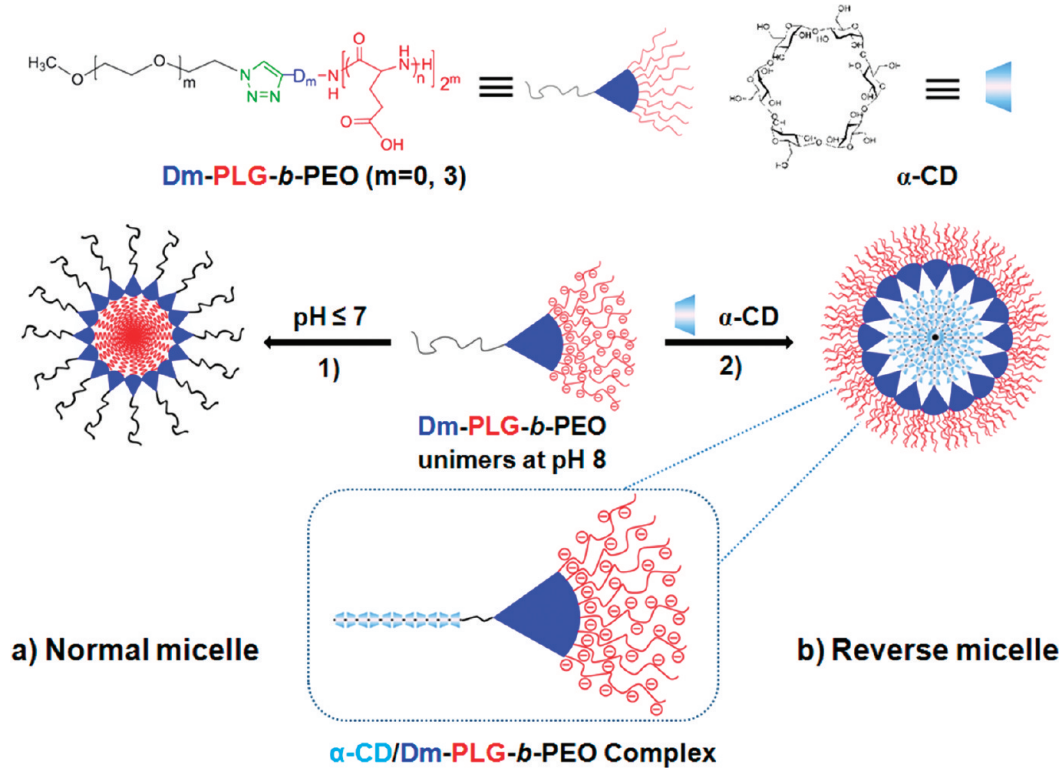

[a] Stages: (1) the micellization of copolymer in neutral or acidic solution; (2) the reverse micellization of copolymer after adding α-CD in alkaline solution.

oughly characterized, and the polypeptide-cored normal micelles (i.e., the micelles with a PLG core and a PEO shell) were induced by the hydrogen-bonding interactions among the PLG segments. Importantly, a novel class of polypeptide-shelled reverse micelles (i.e., the micelles with an anionic PLG shell and an α-CD/PEO polypseudorotaxane core) was for the first time generated by host−guest-chemistry-mediated self-assembly of these copolymers and α-CD,[51] which was evidenced by means of UV−vis, DLS, fluorescence spectroscopy, WAXD, DSC, NMR, and TEM. In addition, the in vitro controlled drug-release behavior of the anticancer doxorubicin (DOX)-loaded micelles was studied at aqueous pH 7 and 4 and at 37 °C.

Experimental Section

Materials. α-Cyclodextrin hydrate (α-CD) and pyrene (98%) were purchased from Acros (NJ) and used without further purification. Doxorubicin hydrocloride was purchased from Beijing Huafeng United Technology Corporation (Beijing, China) and used as received. Poly(ethylene glycol) methyl ether (PEO, M_n = 5000, Aldrich) was dried at 50 °C in vacuo overnight before use. According to our previous publications,[49,50] both linear and dendron-like/linear poly(L-glutamic acid)-*b*-poly(ethylene oxide) (Dm-PLG-*b*-PEO, m = 0 and 3) block copolymers with controllable molecular weights and low polydispersities were successfully synthesized by utilizing click chemistry and the ring-opening polymerization of α-amino acid *N*-carboxyanhydride and then followed by the deprotection of poly(γ-benzyl L-glutamate). The molecular characteristics of these Dm-PLG-*b*-PEO copolymers are compiled in Table S1 of the Supporting Information.

Methods. ^{1}H NMR (400 MHz) spectra were performed at room temperature on a Varian Mercury-400 spectrometer. The copolymers were dissolved in D_2O or mixed solvents of CF_3COOD and $CDCl_3$ ($CF_3COOD/CDCl_3$ 1:1 v/v). Molecular weight and polydispersity (M_w/M_n; M_w: weight-average molecular weight, M_n: number-average molecular weight) of the polymer were determined on a gel permeation chromatograph (GPC, Perkin-Elmer Series 200) equipped with two linear Mixed-B columns (Polymer Lab Corporation, pore size: 10 μm, column size: 300 × 7.5 mm) and a refractive index detector (model) at 30 °C. The elution phase was DMF (0.01 mol·L^{-1} LiBr, elution rate: 1.0 mL/min), and polystyrene was used as the calibration standard. Wide-angle X-ray diffraction (WAXD) patterns of powder samples were obtained at room temperature on a Shimadzu XRD-6000 X-ray diffractometer with a Cu Kα radiation source (wavelength = 1.54 Å). The supplied voltage and current were set to 40 kV and 30 mA, respectively. Samples were exposed at a scan rate of $2\theta = 4°$ min^{-1} between $2\theta = 2$ and 40°. Fluorescence spectra were recorded at room temperature using a Perkin-Elmer LS 50B luminescence spectrometer. Pyrene was used as a fluorescence probe at a concentration of 6.0×10^{-7} M. Emission was carried at 390 nm, and excitation spectra were recorded ranging from 220 to 380 nm. The slit widths for both excitation and emission sides were maintained at 3.5 nm. UV−vis spectra of samples were recorded at room temperature using a Spectrumlab54 UV−visible spectrophotometer. The mean size of nanoparticles was determined by dynamic light scattering (DLS) using a Malvern Nano_S instrument (Malvern, U.K.) at 25 °C, and the concentration of sample was 1 mg/mL. All of the measurements were repeated three times, and the average values reported were the mean diameter ± standard deviation. The ζ potential measurements were done with 1 mL of α-CD/Dm-PLG-*b*-PEO complex solution (10 mg/mL) using a Zetasizer Nano ZS90 instrument

(Malvern, U.K.) and Zetasizer software (version 6.01) for data analysis. Transmission electron microscopy (TEM) was performed using a JEM-2010/INCA OXFORD TEM (JEOL/OXFORD) at a 200 kV accelerating voltage. Samples were deposited onto the surface of 300 mesh Formvar-carbon film-coated copper grids. Excess solution was quickly wicked away with a filter paper. The image contrast was enhanced by negative staining with phosphotungstic acid (0.5 wt %).

Normal Micelles Fabrication. The representative procedure for the normal micelles formation is as follows. PLG_{35}-*b*-PEO copolymer (3 mg) was completely dissolved in 2 mL of distilled water at pH 7 in a 5 mL vial. Upon vigorous stirring for 1 h at 25 °C, a bluish tinge characteristic of micellar solutions appears. The pH of the micellar solution is tuned by the addition of NaOH, HCl, or both.

Reverse Micelles Fabrication. The representative procedure for the reverse micelles formation is as follows. PLG_{35}-*b*-PEO copolymer (1.5 mg) was completely dissolved in 1 mL of distilled water at pH 8 (less amount of NaOH was added) in a 5 mL vial, and then 9 mg of α-CD (α-CD × 1, α-CD/EO 1:2 mol/mol) was added under vigorous stirring, followed by sonication for 30 min. The solution turned turbid and was incubated at 25 °C for 12 h.

DOX-Loaded Micelles. Using a dialysis method, the general protocol for the DOX-loaded micelles formation is exemplified by the following procedure. D3-PLG_{13}-*b*-PEO copolymer (10 mg) and doxorubicin hydrochloride (5 mg, 8.6 μmoL) were dissolved in 7.5 mL of DMF, in which 1.5 fold of Et_3N (12.9 μmoL) was added to neutralize HCl in solution. Distilled water (1 mL) was then added gradually at a speed of 30 μL/min using a microsyringe until the formation of nanoparticles. The nanoparticle solution was put in a dialysis bag and subjected to dialysis against 4 × 1 L of distilled water for 24 h. The drug-loaded nanoparticle solution was lyophilized and stored at 4 °C. The drug-loaded nanoparticles (1 mg) were dissolved in 5 mL of DMF and then analyzed by UV absorbance at 500 nm. The drug loading capacity of nanoparticles is calculated as the weight ratio of actual drug to drug-loaded nanoparticles, and the drug loading efficiency of nanoparticles is calculated as the weight ratio of actual and added drug content.

In Vitro DOX Release. The lyophilized DOX-loaded nanoparticles (4 mg) were directly immersed in 1 mL of distilled water (or 0.1 M acetate buffer, pH 4.0) and then put into a dialysis bag. The dialysis bag was put in 15 mL of distilled water (or 0.1 M acetate buffer, pH 4.0) at 37 °C. The drug-released solution was changed periodically, and the amount of DOX released from nanoparticles was determined by measuring the UV−vis absorbance at 500 nm and at room temperature. All release experiments were carried out in duplicate, and all data were averages of six determinations used for drawing Figures.

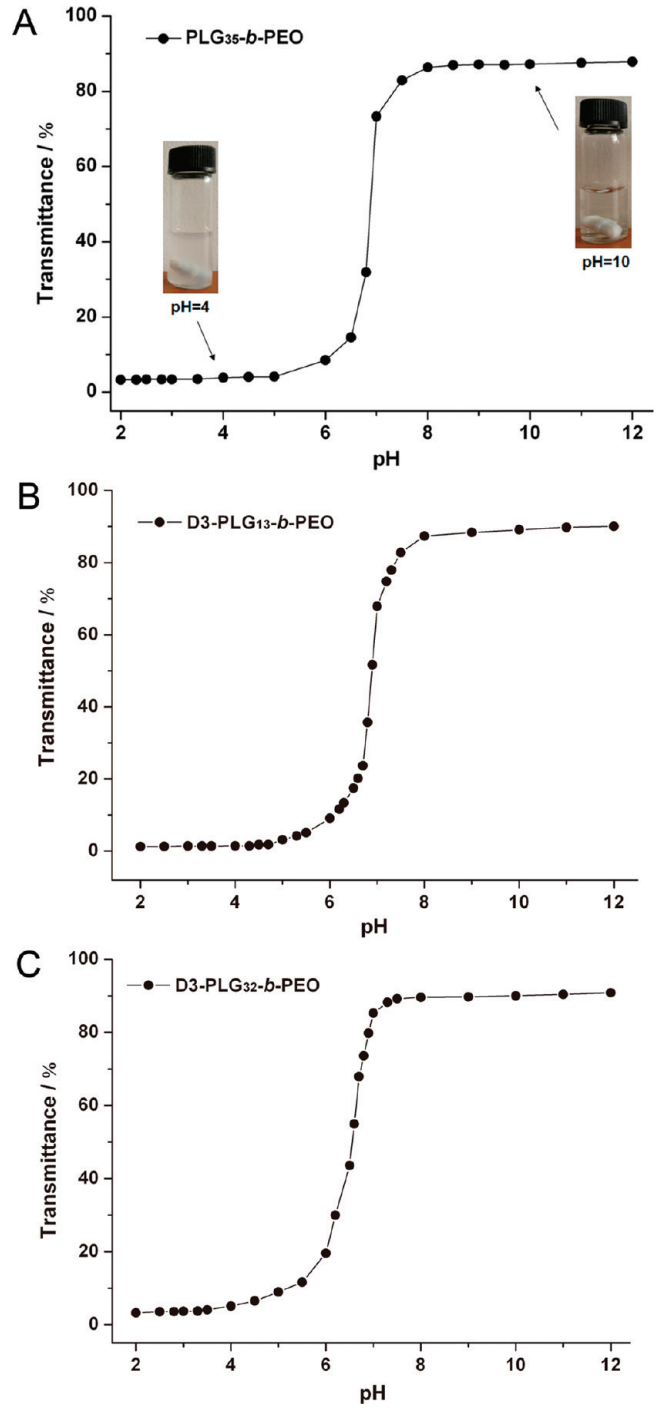

Figure 1. Transmittance of the copolymer solution dependence on pH (inset is the digital photograph).

Results and Discussion

pH-Sensitive Self-Assembly of the Dm-PLG-*b*-PEO Block Copolymers: the Polypeptide-Cored Normal Micelles. In this article, both linear and dendron-like/linear poly(L-glutamic acid)-*b*-poly(ethylene oxide) (Dm-PLG-*b*-PEO, $m = 0$ and 3) block copolymers with controlled molecular weights and low polydispersities were successfully synthesized by using click chemistry according to our previous publication.[49,50] The molecular characteristics of these copolymers are shown in Table S1 of the Supporting Information.

Linear PLG homopolymer ($pK_a = 4.32$) dissolves in water above pH 8 as a weak anionic polyelectrolyte but precipitates from water below pH 4.3, exhibiting a coil−helix conformation transition at pH 5.2.[39,50,52] Therefore, both linear and dendron-like/linear Dm-PLG-*b*-PEO block copolymers are expected to aggregate into nanoparticles under different pH conditions. The pH-mediated self-assembly of these block copolymers was first examined by UV−vis spectroscopy, as shown in Figure 1. The copolymer suspension turned transparent above pH 8 and gave a constant light transmittance of ~90%; whereas it became cloudy and the light transmittance decreased to about 5% below pH 5, suggesting the micellization of Dm-PLG-*b*-PEO in neutral and/or acidic solution (pH ≤ 7). This is attributed to the intermolecular hydrogen-bonding interactions among PLG segments and the resulting insolubility of PLG in neutral and acidic

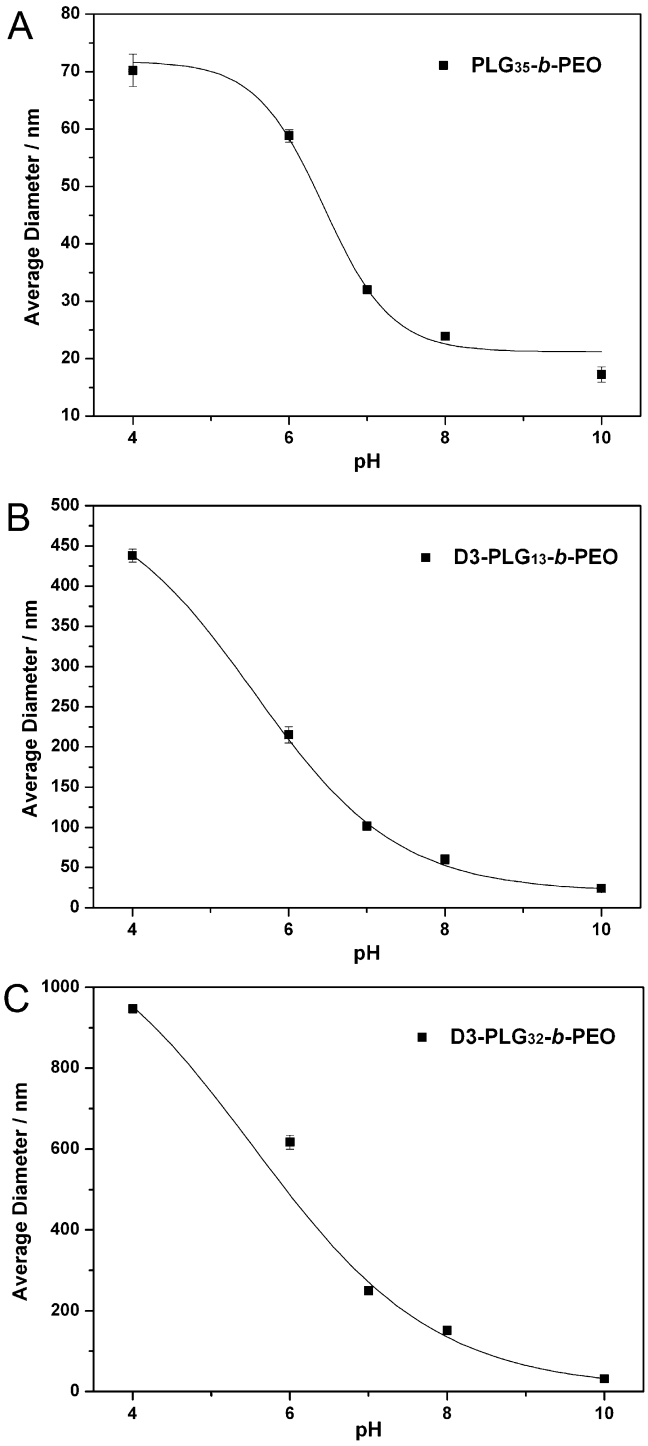

Figure 2. Average size of the self-assembled micelles dependence on pH.

solutions, which induced the microphase separation between PLG and PEO.[39,40,50,52] The self-assembled micelles should have an associated PLG core surrounded by a hydrophilic PEG shell; here we denote the polypeptide-cored micelles as the normal micelles, as illustrated in Scheme 1. Similarly, this pH-sensitive self-assembly was evidenced by DLS and ^{1}H NMR spectroscopy, respectively. As shown in Figure 2, the average size of the normal micelles gradually decreased with the increasing pH value, and the copolymer above pH 8 existed as a unimer basically. This is attributable to the facts that the intermolecular hydrogen-bonding interactions within the PLG segments decreased gradually, whereas the electrostatic repulsion within the

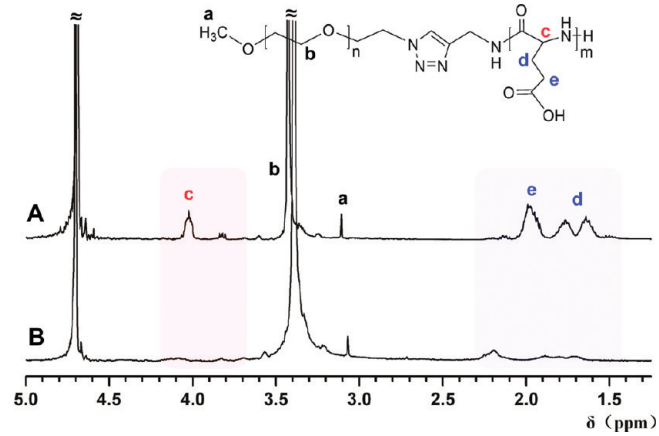

Figure 3. ^{1}H NMR spectra of the copolymer in aqueous solution of pH (A) 10 and (B) 4.

anionic and coiled PLG segments increased reversely.[39,40,50,52] Note that the dendron-like/linear copolymer formed the bigger micelles in solution than the linear counterpart. This is probably attributed to both the stronger intermolecular hydrogen-bonding interactions and the inner cavity among the dendritic PLG core.[48−50,53] In addition, ^{1}H NMR spectroscopy was used to characterize the self-assembled micelles of the copolymer (Figure 3). Compared with that at pH 10, the ^{1}H NMR of copolymer at pH 4 showed the greatly attenuated proton signals of PLG segments. This phenomenon is attributable to both the decreased mobility of the associated PLG core and the shielding effect of PEO shell to the core.

We further confirmed the micellization of the Dm-PLG-*b*-PEO copolymers by examining their critical micelle concentrations (CMCs) using fluorescence spectroscopy (Figure 4), which is an important parameter for characterizing the thermodynamic stability of self-assembled micelles in aqueous solution.[6−9] The fluorescence−excitation spectra of pyrene probe in copolymer at different concentrations are shown in Figure 4A,C. The (0,0) absorption band of pyrene shifted from 335 to 340 nm as the copolymer concentration increased. The red shift is induced by the transfer of pyrene molecules from water to the hydrophobic region, suggesting the micellization of copolymer.[9] The intensity ratio of the bands at 340 and 335 nm (i.e., I_{340}/I_{335}) as a function of the logarithm of the copolymer concentration are shown in Figure 4B,D. The I_{340}/I_{335} ratio remained constant below a certain copolymer concentration; then, it increased substantially, reflecting the incorporation of pyrene in the hydrophobic region of micelles. The CMC of the dendron-like/linear D3-PLG$_{13}$-*b*-PEO copolymer was 0.0071 mg/mL, which was much lower than that of the linear PLG$_{35}$-*b*-PEO copolymer (0.293 mg/mL). This result indicates that the self-assembled micelles of D3-PLG$_{13}$-*b*-PEO are thermodynamically more stable than those of PLG$_{35}$-*b*-PEO, suggesting that the dendritic topology of the polypeptide PLG block is beneficial for the stability of the micelles in aqueous solution.[6−8,48,54−56]

Therefore, do both the aqueous pH and the copolymer topology affect the morphology of the self-assembled micelles? As for the linear PLG$_{35}$-*b*-PEO copolymer with a high PEO composition of ∼52%, the nearly spherical micelles were generated in acidic solution of pH 4, in neutral solution of pH 7, or both (Figure 5A,B). This indicates that pH (≤7) had no apparent effect on the morphology of the self-assembled micelles. Interestingly, the dendron-like/linear D3-PLG$_{13}$-*b*-PEO copolymer with a low PEO composition of ∼25% gave the polydisperse spherical micelles in neutral solution (Figure 5C).

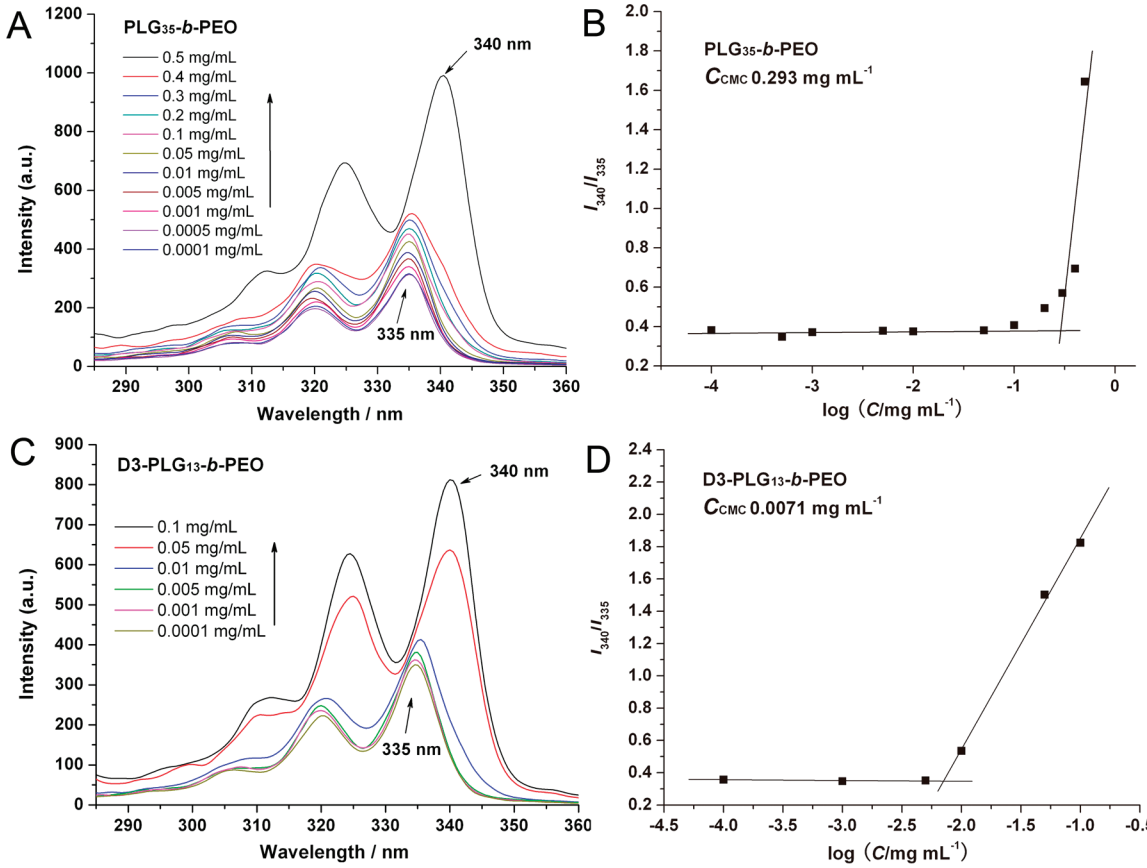

Figure 4. (A) Fluorescence emission spectra of pyrene in the copolymer solution. (B) Plots of I_{340}/I_{335} as a function of the copolymer concentration.

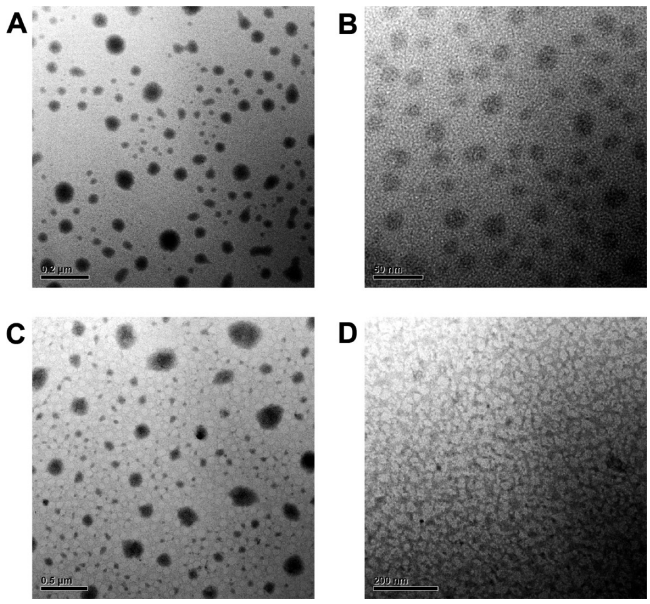

Figure 5. TEM photographs of the normal micelles generated from the copolymer: (A) PLG_{35}-*b*-PEO at pH 4; (B) PLG_{35}-*b*-PEO at pH 7; (C) D3-PLG_{13}-*b*-PEO at pH 7; and (D) D3-PLG_{32}-*b*-PEO at pH 7.

This result is different from the traditional amphiphilic diblock copolymers with a low hydrophilic composition, which often self-assemble into the polymersomes and vesicles with a low curvature.[6−8,27] This is attributable to the fact that the low density of PEO corona connected by the dendritic PLG core decreased the repulsion among the corona chains, stabilizing the micelles with a high curvature.[6−8,27] However, the D3-PLG_{32}-*b*-PEO copolymer with a lower PEO composition of ~13% presented the wormlike micelles in neutral solution (Figure 5D), which is induced by the increased hydrophobicity/hydrophilicity balance.[6−8,27] Taken together, these results demonstrated that both linear and dendron-like/linear Dm-PLG-*b*-PEO block copolymers presented a pH-sensitive self-assembly behavior, and both the copolymer topology and the copolymer composition controlled the morphology of the polypeptide-cored normal micelles. This also provides a convenient method for the fabrication of the polypeptide-cored micelles having a broad composition of hydrophilic PEO in aqueous solution.

Host−Guest Chemistry Mediated the Self-Assembly of the Dm-PLG-*b*-PEO Block Copolymers in Alkaline Solution: The Polypeptide-Shelled Reverse Micelles. From the above results, it can be reasoned that the Dm-PLG-*b*-PEO copolymers exist basically as a unimer in alkaline solution (above pH 8), in which the PLG segment mainly exists as an anionic polyelectrolyte. It is known that α-CD molecules can thread onto the PEO chains to form a crystalline α-CD/PEO polypseudorotaxane.[14−17] Therefore, do these copolymers self-assemble into nanoparticles with the aid of α-CD molecules in alkaline solution? After the addition of a different amount of α-CD to the copolymer solution at pH 10, the original transparent solution turned cloudy, suggesting the micellization of the α-CD/copolymer complex (Figure 6). Meanwhile, the average size of the self-assembled micelles increased from about 113 to 383 nm over the added amount of α-CD, which is probably attributed to the increasing aggregation numbers for the associated α-CD/copolymer complexes.[6−8] Moreover, the CMC of the α-CD/D3-PLG_{13}-*b*-PEO complex (0.03 mg/mL) was lower than that of the α-CD/PLG_{35}-*b*-PEO complex (1.044 mg/mL), suggesting that the dendritic PLG-shelled micelles was

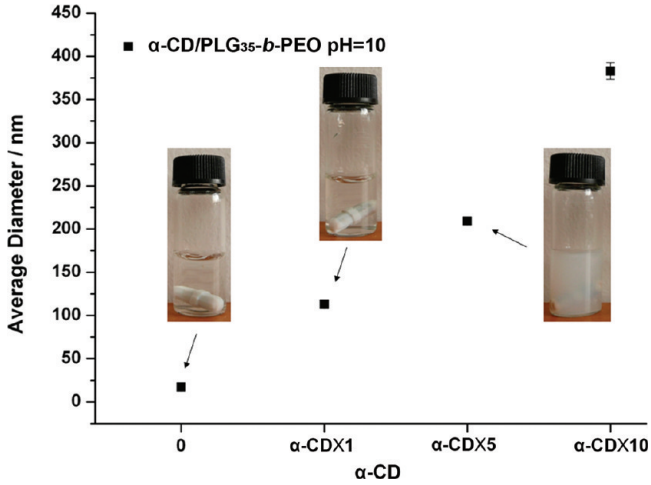

Figure 6. Average size of the reverse micelles from the α-CD/copolymer complex dependence on the amount of α-CD (inset is the digital photograph, $C = 2$ mg/mL).

thermodynamically more stable than the linear counterpart (Supporting Information, Figure S1). The above results indicate that the inclusion complexation between α-CD and the PEO block occurred, and the anionic PLG-shelled micelles with an α-CD/PEO polypseudorotaxane core formed during this process (Scheme 1). Compared with the aforementioned normal micelles (i.e., the micelles with a PEO shell and a PLG core), we denote these as the reverse micelles (i.e., the micelles with an anionic PLG shell and an α-CD/PEO polypseudorotaxane core), a term coined by Armes et al.[51] Furthermore, the inclusion complexation of Dm-PLG-*b*-PEO and α-CD was confirmed by both WAXD and DSC techniques. After α-CD molecules threading onto the PEO backbone, a strong new diffraction peak at 1.40 $Å^{-1}$ appeared for the crystalline α-CD/PEO polypseudorotaxane, as demonstrated by Figure 7A. This was also concomitant with the disappearance of diffraction peaks at 1.34 and 1.64 $Å^{-1}$ for the PEO block. The DSC analysis indicates that the crystallization of PEO block was completely suppressed within the α-CD cavities (Figure 7B), suggesting that the PEO backbone was threaded by α-CD molecules.[9,10] In addition, the ^{1}H NMR analysis confirmed that the host−guest stoichiometry (i.e., EO/α-CD, mol/mol) was about 2 for the α-CD/copolymer complex (Supporting Information, Figure S2). This is consistent with the theoretical value of the host−guest stoichiometry,[14−17] demonstrating that the repeating EO units within copolymer were completely threaded by α-CD molecules.

Indeed, do the reverse micelles have an anionic PLG shell? The ζ potential of the reverse micelles ranged from −20.2 to −24.2 mV (Supporting Information, Figure S3), demonstrating that the reverse micelles have an anionic PLG shell. The linear α-CD/PLG_{35}-*b*-PEO complex showed the nearly spherical micelles, whereas the dendron-like/linear α-CD/D3-PLG_{13}-*b*-PEO complex mainly self-assembled into the worm-like micelles (Figure 8). Taken together, these results convincingly confirmed that the inclusion complexation between Dm-PLG-*b*-PEO and α-CD in alkaline solution drove the self-assembly and generated the reverse micelles, as shown in Scheme 1. To the best of our knowledge, this is a first example of the fabrication of the polypeptide-shelled micelles by utilizing host−guest chemistry.[14−46]

In Vitro Anticancer Drug Release Behavior of Doxorubicin-Loaded Micelles. The hydrophobic DOX induces apoptosis by intercalating with DNA, making it widely used in clinical cancer chemotherapy.[57,58] Using a dialysis method,[55] we successfully loaded DOX into the copolymer micelles, and the

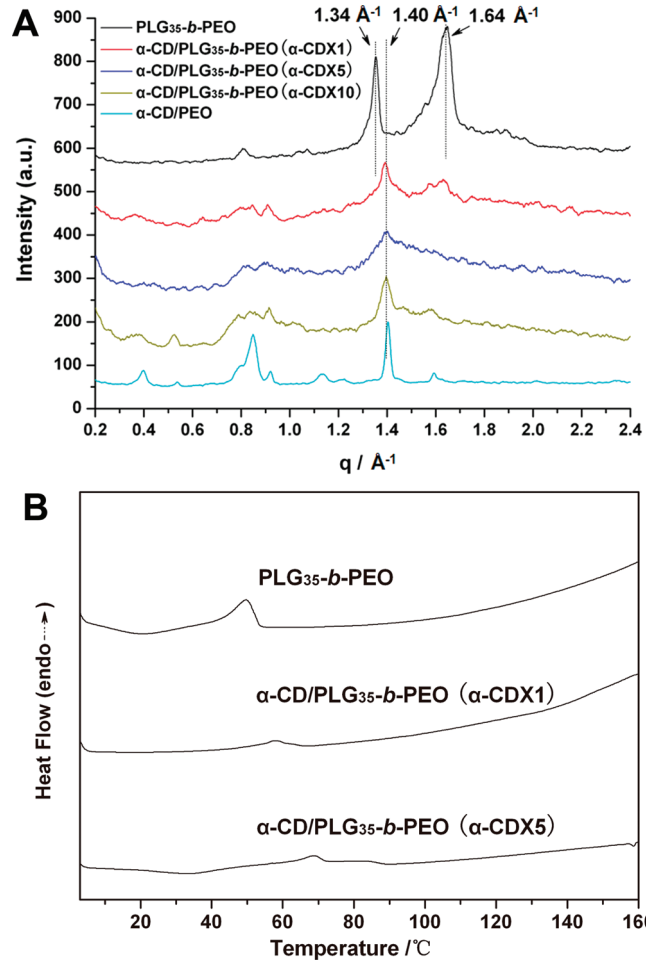

Figure 7. (A) WAXD patterns for the α-CD/copolymer complex and copolymer. (B) DSC curves for the α-CD/copolymer complex and copolymer in the second heating run.

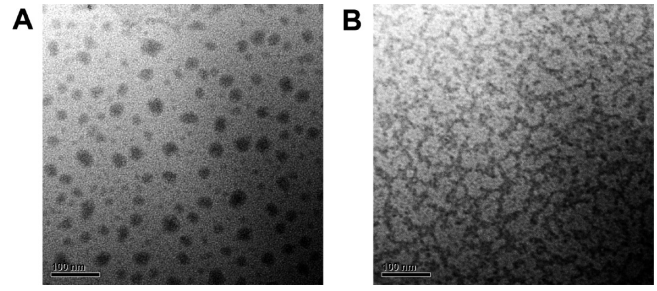

Figure 8. TEM photographs of the reverse micelles from the α-CD/copolymer complex: (A) α-CD/PLG_{35}-*b*-PEO and (B) α-CD/D3-PLG_{13}-*b*-PEO.

related DOX-loaded micelles were characterized by TEM (Figure 9). Compared with the blank spherical micelles (Figure 5B), the wormlike micelles with few spherical micelles were obtained for the DOX-loaded micelles fabricated from the linear PLG_{35}-*b*-PEO copolymer (Figure 9 A). This is attributable to the hydrophobic DOX molecules loaded within micelles, resulting in the increased hydrophobicity/hydrophilicity balance.[6−8,27] Similarly, in comparison with the blank and spherical micelles (Figure 5C), the DOX-loaded micelles fabricated from the dendron-like/linear D3-PLG_{13}-*b*-PEO copolymer presented the rigid wormlike or rod micelles. This is due to the higher DOX loading content (see below), resulting in the higher hydrophobicity/hydrophilicity balance.[6−8,27] Therefore, these results indicate that the loaded hydrophobic DOX molecules regulated

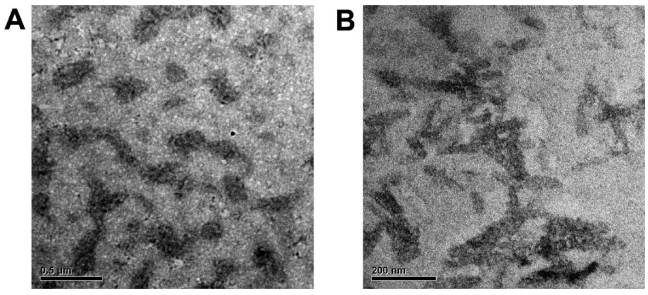

Figure 9. TEM photographs of the doxorubicin-loaded micelles from (A) PLG_{35}-*b*-PEO and (B) D3-PLG_{13}-*b*-PEO.

the hydrophobicity/hydrophilicity balance of the copolymer matrix, resulting in the worm-like micelles with a lower curvature than the spherical micelles. Note that the worm-like DOX-loaded micelles might be a better anticancer vesicle than the spherical micelles, as reported by Discher et al.[59]

The DOX loading efficiency of the dendron-like/linear D3-PLG_{13}-*b*-PEO copolymer was ~38%, higher than that (~19%) for the linear PLG_{35}-*b*-PEO copolymer. Meanwhile, the DOX loading capacity is about 24 and 13% for the dendron-like/linear and the linear copolymers, respectively. These results suggest that the dendron-like/linear copolymer might provide both the interior cavity and the larger space among the dendritic core for the encapsulation of DOX.[48,53,55] The in vitro drug-release behavior of the DOX-loaded micelles in aqueous solution (pH 7 and 4) at 37 °C is shown in Figure 10. The drug-release profile of the D3-PLG_{13}-*b*-PEO copolymer micelles at pH 7 showed a triphasic pattern,[55,60] that is, with a fast drug-release rate (K_1 = 0.43 h^{-1}) within the initial 40 h (i.e., ~20% of drug was released), a moderate drug-release rate (K_2 = 0.08 h^{-1}) within ~220 h (i.e., ~20% of drug was released), followed by a slow drug-release rate (K_3 = 0.03 h^{-1}) within the next 1380 h (i.e., ~42% of drug was released). The initial burst release is attributable to the fact that DOX was probably encapsulated in the surface layer of associated PLG core, and that the drug-loaded micelles had large surface areas.[55,61] Meanwhile, the associated polypeptide PLG core within the DOX-loaded micelles should not degrade at pH 7, suggesting that the degradation-induced drug release can be negligible.[3,4,62] Therefore, the following DOX release was mainly controlled by the drug diffusion from micelles, which was associated with enhanced water uptake by hydrophilic PEO corona at 37 °C. As for the linear PLG_{35}-*b*-PEO copolymer micelles, the drug release profile gave a similar triphasic pattern, that is, with a fast drug-release rate (K_1' = 1.77 h^{-1}) within the initial 10 h (i.e., ~30% of drug was released), a moderate drug-release rate (K_2' = 0.27 h^{-1}) within ~90 h (i.e., ~26% of drug was released), followed by a slow drug-release rate (K_3' = 0.04 h^{-1}) within the next 620 h (i.e., ~25% of drug was released). In addition, the DOX-loaded micelles at pH 4 showed a much faster drug-release rate than those at pH 7, which is due to the increased aqueous solubility of DOX in acidic solution.[55,57] Taken together, all results demonstrate that the copolymer topology obviously affected both the drug-loading efficiency (and/or capacity) and the drug-release rate of DOX-loaded micelles, and the DOX-loaded micelles fabricated from the dendron-like/linear copolymer sustained a longer drug-release time than those of the linear counterpart. Note that the reverse micelles were fabricated under basic condition (pH 8) and would precipitate under neutral or acidic conditions (e.g., at pH 7 and/or pH 4). Therefore, the reverse micelles cannot be used as the nanocarrier for drug-release under physiological conditions.

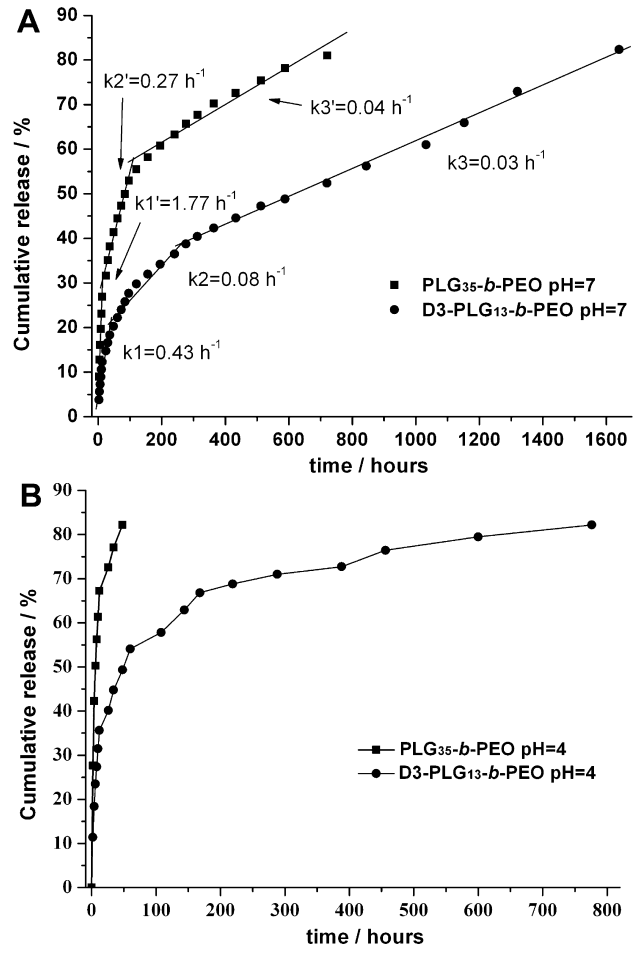

Figure 10. In vitro drug-release profile of doxorubicin-loaded micelles from PLG_{35}-*b*-PEO and D3-PLG_{13}-*b*-PEO at 37 °C: (A) pH 7 and (B) 4.

Conclusions

Both the polypeptide-cored normal micelles and the polypeptide-shelled reverse micelles were successfully fabricated from the Dm-PLG-*b*-PEO copolymers via hydrogen-bonding interactions or host−guest chemistry. These linear and dendron-like/linear block copolymers presented a pH-sensitive self-assembly in aqueous solution, which was mediated by the intermolecular hydrogen-bonding interactions among PLG segments. Meanwhile, both the copolymer topology and the composition controlled the morphology (spherical and wormlike) of the normal micelles. Significantly, the polypeptide-shelled reverse micelles were first introduced and generated by host−guest-chemistry-mediated self-assembly of these copolymers and α-CD, and the ζ potential analysis confirmed that the reverse micelles had an anionic PLG shell. In addition, the DOX-loaded micelles fabricated from the dendron-like/linear copolymer gave a higher DOX loading efficiency and capacity and sustained a longer drug-release period than the linear counterpart, potentially making them useful for the anticancer drug delivery systems.

Acknowledgment. We are grateful for the financial support of National Natural Science Foundation of China (20874058 and 20674050), Shanghai Leading Academic Discipline Project (B202), and SJTU excellent young faculty project (T241460638). The assistance of Instrumental Analysis Center of SJTU is also appreciated.

Supporting Information Available: Molecular characteristics for Dm-PLG-*b*-PEO, NMR, CMC, and ζ potential curves.

This material is available free of charge via the Internet at http://pubs.acs.org.

References and Notes

(1) Meng, F.; Zhong, Z.; Feijen, J. *Biomacromolecules* **2009**, *10*, 197–209.
(2) Wei, H.; Cheng, S. X.; Zhang, X. Z.; Zhuo, R. X. *Prog. Polym. Sci.* **2009**, *34*, 893–910.
(3) Bae, Y.; Kataoka, K. *Adv. Drug Delivery Rev.* **2009**, *61*, 768–784.
(4) Osada, K.; Kataoka, K. *Adv. Polym. Sci.* **2006**, *202*, 113–153.
(5) Batrakova, E. V.; Kabanov, A. V. *J. Controlled Release* **2008**, *130*, 98–106.
(6) Discher, D. E.; Ortiz, V.; Srinivas, G.; Klein, M. L.; Kim, Y.; Christian, D.; Cai, S.; Photos, P.; Ahmed, F. *Prog. Polym. Sci.* **2007**, *32*, 838–857.
(7) Discher, D. E.; Ahmed, F. *Annu. Rev. Biomed. Eng.* **2006**, *8*, 323–341.
(8) Discher, D. E.; Eisenberg, A. *Science* **2002**, *297*, 967–973.
(9) Zhang, J.; Ma, P. X. *Angew. Chem., Int. Ed.* **2009**, *48*, 964–968.
(10) Xu, J.; Liu, S. Y. *Soft Matter* **2008**, *4*, 1745–1749.
(11) Zou, J.; Tao, F.; Jiang, M. *Langmuir* **2007**, *23*, 12791–12794.
(12) Wang, Y. P.; Ma, N.; Wang, Z. Q.; Zhang, X. *Angew. Chem., Int. Ed.* **2007**, *46*, 2823–2826.
(13) Hofmeier, H.; Schubert, U. S. *Chem. Commun.* **2005**, 2423–2432.
(14) Li, J. *Adv. Polym. Sci.* **2009**, *222*, 79–113.
(15) Wu, Y. L.; Li, J. *Angew. Chem., Int. Ed.* **2009**, *48*, 3842–3845.
(16) Harada, A.; Takashima, Y.; Yamaguchi, H. *Chem. Soc. Rev.* **2009**, *38*, 875–882.
(17) Harada, A.; Hashidzume, A.; Yamaguchi, H.; Takashima, Y. *Chem. Rev.* **2009**, *109*, 5974–6023.
(18) Choi, S. W.; Amajjahe, S.; Ritter, H. *Adv. Polym. Sci.* **2009**, *222*, 175–203.
(19) Yui, N.; Katoono, R.; Yamashita, A. *Adv. Polym. Sci.* **2009**, *222*, 55–77.
(20) Li, J.; Loh, X. J. *Adv. Drug Delivery Rev.* **2008**, *60*, 1000–1017.
(21) Yang, C.; Li, J. *J. Phys. Chem. B* **2009**, *113*, 682–690.
(22) Dai, X. H.; Dong, C. M.; Yan, D. *J. Phys. Chem. B* **2008**, *112*, 3644–3652.
(23) Dong, H. Q.; Li, Y. Y.; Cai, S. J.; Zhuo, R. X.; Zhang, X. Z.; Liu, L. J. *Angew. Chem., Int. Ed.* **2008**, *47*, 5573–5576.
(24) Reynhout, I. C.; Cornelissen, J. J. L. M.; Nolte, R. J. M. *Acc. Chem. Res.* **2009**, *42*, 681–692.
(25) Gauthier, M. A.; Klok, H. A. *Chem. Commun.* **2008**, 2591–2611.
(26) Hamley, I. W. *Angew. Chem., Int. Ed.* **2007**, *46*, 8128–8147.
(27) Van Dongen, S. F. M.; De Hoog, H. P. M.; Peters, R. J. R. W.; Nallani, M.; Nolte, R. J. M.; Van Hest, J. C. M. *Chem. Rev.* **2009**, *109*, 6212–6274.
(28) Lowik, D. W. P. M.; Ayres, L.; Smeenk, J. M.; Van Hest, J. C. M. *Adv. Polym. Sci.* **2006**, *202*, 19–52.
(29) Schlaad, H. *Adv. Polym. Sci.* **2006**, *202*, 53–73.
(30) Klok, H. A.; Lecommandoux, S. *Adv. Polym. Sci.* **2006**, *202*, 75–111.
(31) Zhao, X.; Zhang, S. *Adv. Polym. Sci.* **2006**, *203*, 145–170.
(32) Zhang, X.; Li, J.; Li, W.; Zhang, A. *Biomacromolecules* **2007**, *8*, 3557–3567.
(33) Li, J.; Wang, T.; Wu, D.; Zhang, X.; Yan, J.; Du, S.; Guo, Y.; Wang, J.; Zhang, A. *Biomacromolecules* **2008**, *9*, 2670–2676.
(34) Rao, J.; Luo, Z.; Ge, Z.; Liu, H.; Liu, S. *Biomacromolecules* **2007**, *8*, 3871–3878.
(35) Guo, Z.; Li, Y.; Tian, H.; Zhuang, X.; Chen, X.; Jing, X. *Langmuir* **2009**, *25*, 9690–9696.
(36) Sun, J.; Deng, C.; Chen, X.; Yu, H.; Tian, H.; Sun, J.; Jing, X. *Biomacromolecules* **2007**, *8*, 1013–1017.
(37) Gebhardt, K. E.; Ahn, S.; Venkatachalam, G.; Savin, D. A. *Langmuir* **2007**, *23*, 2851–2856.
(38) Sallach, R. E.; Wei, M.; Biswas, N.; Conticello, V. P.; Lecommandoux, S.; Dluhy, R. A.; Chaikof, E. L. *J. Am. Chem. Soc.* **2006**, *128*, 12014–12019.
(39) Rodriguez-Hernandez, J.; Lecommandoux, S. *J. Am. Chem. Soc.* **2005**, *127*, 2026–2027.
(40) Checot, F.; Brulet, A.; Oberdisse, J.; Gnanou, Y.; Mondain-Monval, O.; Lecommandoux, S. *Langmuir* **2005**, *21*, 4308–4315.
(41) Bellomo, E.; Wyrsta, M. D.; Pakstis, L.; Pochan, D. J.; Deming, T. J. *Nat. Mater.* **2004**, *3*, 244–248.
(42) Cai, C.; Zhang, L.; Lin, J.; Wang, L. *J. Phys. Chem. B* **2008**, *112*, 12666–12673.
(43) Ding, W.; Lin, S.; Lin, J.; Zhang, L. *J. Phys. Chem. B* **2008**, *112*, 776–783.
(44) Qiu, S.; Huang, H.; Dai, X. H.; Zhou, W.; Dong, C. M. *J. Polym. Sci., Polym. Chem.* **2009**, *47*, 2009–2023.
(45) Dong, C. M.; Chaikof, E. L. *Colloid Polym. Sci.* **2005**, *283*, 1366–1370.
(46) Dong, C. M.; Sun, X. L.; Faucher, K. M.; Apkarian, R. P.; Chaikof, E. L. *Biomacromolecules* **2004**, *5*, 224–231.
(47) Jabr-Milane, L.; Van Vlerken, L.; Devalapally, H.; Shenoy, D.; Komareddy, S.; Bhavsar, M.; Amiji, M. *J. Controlled Release* **2008**, *130*, 121–128.
(48) Haag, R. *Angew. Chem., Int. Ed.* **2004**, *43*, 278–282.
(49) Peng, S. M.; Chen, Y.; Hua, C.; Dong, C. M. *Macromolecules* **2009**, *42*, 104–113.
(50) Chen, Y.; Pang, X. H.; Dong, C. M. *Adv. Funct. Mater.* **2010**, *20*, 579–586.
(51) The term "reverse micelles" was coined by Armes et al., see references: (a) Liu, S.; Billingham, N. C.; Armes, S. P. *Angew. Chem., Int. Ed.* **2001**, *40*, 2328–2331. (b) Butun, V.; Billingham, N. C.; Armes, S. P. *J. Am. Chem. Soc.* **1998**, *120*, 11818–11819.
(52) Kukula, J.; Schlaad, H.; Antonietti, M.; Forster, S. *J. Am. Chem. Soc.* **2002**, *124*, 1658–1663.
(53) Svenson, S.; Tomalia, D. A. *Adv. Drug Delivery Rev.* **2005**, *57*, 2106–2129.
(54) Hua, C.; Peng, S. M.; Dong, C. M. *Macromolecules* **2008**, *41*, 6686–6695.
(55) Yang, Y.; Hua, C.; Dong, C. M. *Biomacromolecules* **2009**, *10*, 2310–2318.
(56) Dai, X. H.; Dong, C. M. *J. Polym. Sci., Polym. Chem.* **2008**, *46*, 817–829.
(57) Gillies, E. R.; Fréchet, J. M. J. *Bioconjugate Chem.* **2005**, *16*, 361–368.
(58) Kwon, G.; Naito, M.; Yokoyama, M.; Okano, T.; Sakurai, Y.; Kataoka, K. *J. Controlled Release* **1997**, *48*, 195–201.
(59) Geng, Y.; Dalhaimer, P.; Cai, S.; Tsai, R.; Tewari, M.; Minko, T.; Discher, D. E. *Nature Nanotechnol.* **2007**, *2*, 249–255.
(60) Bertin, P. A.; Smith, D. D.; Nguyen, S. T. *Chem. Commun.* **2005**, 3793–3795.
(61) Dong, Y.; Feng, S. S. *J. Biomed. Mater. Res.* **2006**, *78A*, 12–19.
(62) Dong, C. M.; Guo, Y. Z.; Qiu, K. Y.; Gu, Z. W.; Feng, X. D. *J. Controlled Release* **2005**, *107*, 53–64.

JP100399D